

# SIZE EFFECT IN CONCRETE COLUMNS: FINITE-ELEMENT ANALYSIS WITH MICROPLANE MODEL

By Michele Brocca<sup>1</sup> and Zdeněk P. Bažant,<sup>2</sup> Fellow, ASCE

**ABSTRACT:** Failure of concrete structures due to concrete failing in compression was recently shown to exhibit a size effect. This is not taken into account by current design codes based on failure criteria expressed in terms of strength or plasticity. But compressive failure of concrete cannot be described by strength criteria, since it is brittle and is caused by release of elastic strain energy stored in the structure. In this sense, it is similar to tensile failure governed by fracture mechanics. The paper presents a finite-element study of the size effect of compressive failure of geometrically similar concrete columns of different sizes. The test columns considered here are reduced-scale specimens made with micro-concrete of maximum aggregate size 3.35 mm and are loaded eccentrically. The analysis employs the microplane model for concrete. It is based on the crack-band concept and is shown to capture with good approximation the size effect observed experimentally.

## INTRODUCTION

The current design codes for reinforced concrete columns, based on failure criteria expressed in terms of strength or yield surfaces, exhibit no size effect, i.e., no dependence of the nominal strength on the size of the structure. (As standard in mechanics, the term “nominal strength” is here used to mean the load divided by the cross-section area, and not the ultimate axial force, as used by ACI. In mechanics, the “strength” always has the dimension of stress.) However, the failure of concrete columns is not plastic, but brittle, as confirmed by the fact that the observed load-deflection diagrams of columns have no yield plateau but descend after the peak. Under extremely high confining pressures (Bažant et al. 1999; Brocca and Bažant 1999), compressive failure of concrete can be ductile, without any significant postpeak decrease of applied load. But such pressures can develop only when the concrete is confined in very strong steel tubes. Thus, the description of structural behavior of concrete in terms of plastic limit states is in general not correct. Mathematical modeling of such behavior should be based on fracture mechanics, which predicts size effect, such that the nominal strength at failure,  $\sigma_N$ , decreases with an increase of the characteristic dimension of the structure,  $D$ , provided that the structures of different sizes are geometrically similar.

In the concrete fracture community, it is now generally accepted that size effects must occur in all the failures of concrete structures that are due to concrete rather than to steel. This is true not only of those failures that are due to concrete failing in tension (punching shear of slabs, torsion, anchor pullout, bar pullout, splice failure, etc.) but also of the failures that are due to concrete failing in compression. This includes the bending of prestressed concrete beams, anchor pullout, and diagonal shear failure of reinforced concrete beams, and all the cases analyzed by the strut-and-tie model, in which failure is due to crushing of the so-called “compression strut” of concrete. Most importantly, this includes reinforced concrete columns, which will be studied in this paper from the size effect viewpoint.

Experimental results documenting a size effect in compres-

sive failure of quasibrittle materials such as concrete, rock, ceramics, and composites can be found, for example, in van Mier (1986), Gonnermann (1925), Blanks and McNamara (1935), Marti (1989), and Jishan and Xixi (1990).

Although the load capacity of reinforced concrete columns is now quite well understood (Nilson and Winter 1986; McGregor 1988; Bažant and Cedolin 1991; Bažant and Xiang 1991; Bažant and Chen 1997; Bažant et al. 1991), the size effect in columns has escaped attention so far. Until about 15 years ago, it had erroneously been believed that all the size effects in concrete structures are totally explicable by the statistical nature of material strength as described by Weibull-type theories. In reality, however, the portion of the size effect ascribable to the randomness of concrete strength is very small and is negligible in structures in which there is large crack growth before the maximum load is reached (Bažant 1984a; Bažant et al. 1991; Bažant and Xi 1991). In such structures, the mean size effect is almost totally deterministic and is caused by the fact that a larger structure stores a greater amount of strain energy; thus, the rate of energy release into an advancing fracture front grows with structure size, while the energy dissipated at the fracture front per unit fracture advance is approximately independent of the structure size. This source of size effect was first recognized for the case of tensile failure, but a similar phenomenon occurs also when the structure fails in compression.

Compressive failure is caused predominantly by the release of stored energy from the structure in a fashion similar to tensile failure, as suggested and implied by several researchers (Hoek and Bieniawski 1965; Cotterrell 1972; Bieniawski 1974; Ingraffea 1977; Bažant et al. 1993). Therefore, the study of size effect in compression must be based on fracture mechanics. A simplified model for the mechanism of compression failure, aimed at the study of the accompanying size effect, is given by Bažant and Xiang (1997), who modeled the lateral propagation of a cracking band assumed to consist of densely distributed axial splitting microcracks.

The objective of this paper is to show how the size effect in concrete columns can be determined through finite-element analysis based on the crack-band model (Bažant and Oh 1983). This will be done by performing a finite-element analysis of a series of reduced-scale laboratory tests conducted at Northwestern University (Bažant and Kwon 1994). In this paper, first the results of a series of tests on small microconcrete columns are reviewed. Then, the approach used for the finite-element analysis is explained. Subsequently, the basic formulation of the microplane model that is employed for the concrete constitutive model is outlined. Finally, the results of the analysis are presented and discussed.

<sup>1</sup>Grad. Res. Asst., Northwestern Univ., Evanston, IL 60208; currently at Boston Consulting Group, Chicago.

<sup>2</sup>Walter P. Murphy Prof. of Civ. Engrg. and Materials Sci., Northwestern Univ., Evanston, IL 60208. E-mail: z-bazant@northwestern.edu

Note. Associate Editor: John Wallace. Discussion open until May 1, 2002. To extend the closing date one month, a written request must be filed with the ASCE Manager of Journals. The manuscript for this paper was submitted for review and possible publication on December 28, 1999; revised May 24, 2001. This paper is part of the *Journal of Structural Engineering*, Vol. 127, No. 12, December, 2001. ©ASCE, ISSN 0733-9445/01/0012-1382-1390/\$8.00 + \$.50 per page. Paper No. 22202.

## EXPERIMENTAL RESULTS

In 1994, Bažant and Kwon presented the results of a series of tests performed on reinforced concrete columns of reduced size made with microconcrete. The purpose of these tests was to show the presence of a significant size effect in compressive failure of columns and to ascertain how the strengths of columns of different sizes are mutually related.

The test specimens (Fig. 1) were tied reinforced concrete columns of square cross sections with sides  $D = 12.7, 25.4,$  and  $50.8$  mm (0.5, 1, and 2 in.). Three column slendernesses,  $\lambda = 19.2, 35.8,$  and  $52.5,$  were used ( $\lambda = L/r,$  and according to ACI,  $r = 0.3D$  for typical reinforced concrete sections). The corresponding effective lengths of the columns, measured between the contact points of the steel balls, were  $L = 73, 136.5,$  and  $200$  mm (2.875, 5.375, and 7.875 in.) for the smallest cross section,  $L = 146, 273,$  and  $400$  mm (5.75, 10.75, and 15.75 in.) for the middle cross section, and  $L = 292, 546,$  and  $800$  mm (11.5, 21.5, and 31.5 in.) for the largest cross section. The loads were applied to the steel platens through steel balls and steel plates.

In each group, the columns of the same slenderness and different cross sections were geometrically similar. To separate the effects of size and the effect of geometry, the geometric similarity was enforced scrupulously: the reinforcing steel bars, their location coordinates and cover, as well as the diameter and spacing of the ties were all scaled in proportion to  $D,$  as defined in Fig. 1. Smooth reinforcing steel bars were used because of the unavailability of properly scaled deformed bars of reduced sizes.

The columns were simply supported and the load  $P$  was applied with eccentricities  $e$  that were geometrically similar:  $e = 0.25D.$  The steel ratio was 4.91%. The Young's modulus of the steel bars was  $E_s = 200$  GPa (29,000 ksi). The specified yield strength was  $f_y = 552$  MPa (80,000 psi). Upon reaching the yield limit, the bars deformed plastically.

The concrete (actually a microconcrete or mortar) was made of Type I portland cement with a water-cement ratio 0.65 (for easy workability). The maximum aggregate size was 3.35 mm (0.132 in.). All the specimens were cast from the same batch of concrete. The average uniaxial compression strength of con-

crete, measured on 76.2 mm (3 in.) diameter, was  $f'_c = 28.96$  MPa (4,200 psi). Note that the aggregate size  $d_a$  was kept constant and not scaled with size  $D.$  This must be so because, if  $d_a$  were changed, one would have a different concrete, with different properties. The known scaling laws for geometrically similar structures of different sizes are valid only when one and the same material is used for all the sizes. Detailed information about the tests can be found in Bažant and Kwon (1994).

The results of the tests are shown in Fig. 2 as the plots of  $\sigma_N$  versus  $\log D,$  which represent the standard size effect plots. The value of the nominal strength  $\sigma_N = P/D^2$  is calculated from the peak loads measured in individual tests. All these plots clearly indicate a strong size effect.

## FINITE-ELEMENT ANALYSIS

The present finite-element analysis of the tests is performed using a three-dimensional explicit finite-element code, geometrically nonlinear, developed with updated Lagrangian formulation. Eight-node brick elements are used for concrete as well as for the steel plates at the top and bottom of the specimen. The reinforcement is modeled with truss elements, and an elastic-plastic law is assumed for steel. Debonding with slip of the reinforcing bars at the nodal points is neglected. The assumption of a perfect bond between concrete and steel at the nodal points is a simplification that might have some effect. This point will be discussed later.

The constitutive law adopted for concrete is the microplane model M4 developed by Bažant et al. (2000b) and Caner and Bažant (2000). In microplane finite-element analysis, damage is modeled as smeared over the domain of the element. When such a smeared approach is used, numerical analysis of compression failure of concrete faces the same difficulties as posed by tensile strain softening. Strain softening, whether tensile or compressive, is known to cause a loss of well-posedness and spurious strain localization into arbitrarily small regions.

This can be easily understood by considering the example of a bar made of a material characterized by an elastic-softening constitutive law (Bažant 1976; Bažant and Planas 1998). If the bar is discretized into  $N$  elements, it can be shown that,

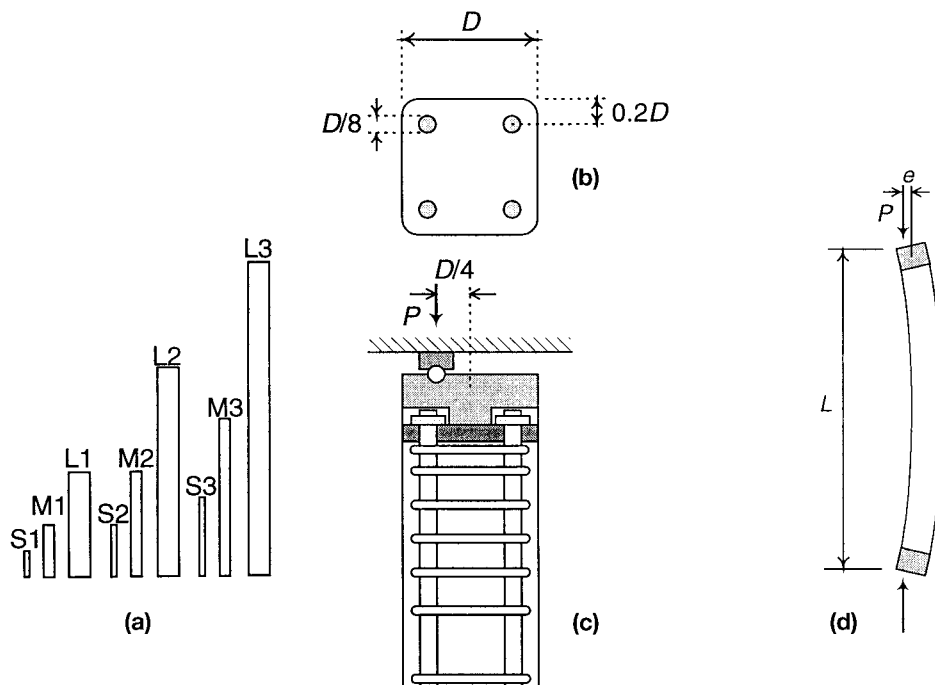


FIG. 1. (a) Column Specimens of Three Different Sizes and Three Different Slendernesses, Tested by Bažant and Kwon (1994); (b) Horizontal Cross Section of Columns; (c) Vertical Cross Section of Columns; (d) Deformation under Eccentric Loading Applied

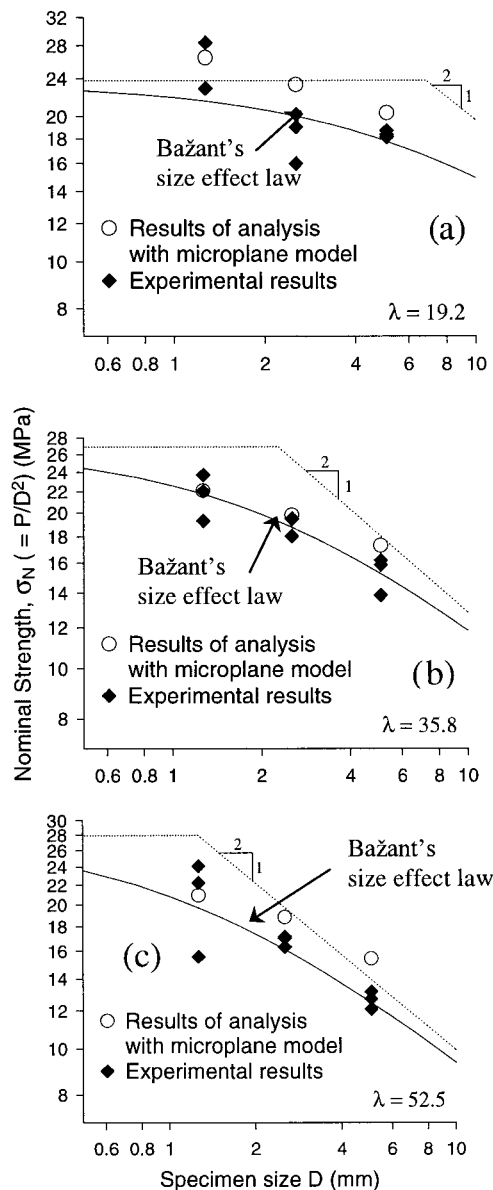


FIG. 2. Calculated Size Effect Plots for Columns of Three Different Slendernesses  $\lambda$ , Compared with Test Data Points from Bažant and Kwon (1994)

after the stress peak, the strain must localize in only one of the elements. Only one element continues deforming at decreasing stress, while the others unload elastically. Thus, the size of the damaged region and the postpeak response of the bar depend on  $N$ . Such a phenomenon is usually referred to as mesh unobjectivity or spurious mesh sensitivity and is obviously unacceptable—conceptually, physically, and computationally. It occurs not only for static but also for dynamic loading (Bažant and Cedolin 1991). The general remedy to this problem is to apply some form of the nonlocal continuum concept (Eringen 1965, 1966; Kröner 1967; Kunin 1968; Levin 1971) to the strain-softening damage, as proposed and developed by Bažant (1984a, 1991, 1994), Bažant et al. (1984), Bažant and Lin (1988a,b), Pijaudier-Cabot and Bažant (1987), Bažant and Pijaudier-Cabot (1988, 1989), Bažant and Ožbolt (1990, 1992), Jirásek and Bažant (1994), Ožbolt and Bažant (1996), Planas et al. (1993, 1994).

In a nonlocal formulation, it is recognized that continuum damage models cannot be implemented with the classical assumption that stress at a point depends only on the strain at the same point. Rather, a more general concept of a nonlocal

continuum must be adopted. In the early nonlocal models, the stress at a point was considered to depend not only on the strain at that point but also on the strain in the neighborhood of that point, or on some kind of average of strain in the neighborhood (although this average may further be approximated by the second strain gradient). In the case of strain softening, this early approach must be modified by considering the stress to depend on the average of only the inelastic part of strain, or the average of some parameters of inelastic strain (Pijaudier-Cabot and Bažant 1987). The nonlocal approach can thus take into account the interaction of microcracks and other microscale sources of damage (Bažant 1991, 1994).

However, even without directly addressing the nonlocality, spurious strain localization can be prevented by introducing some type of strain localization limiter, i.e., a mathematical restriction on the size of the damaged region to be associated with the material constitutive model. A popular and effective way to do so is the crack band model, proposed in general terms by Bažant (1976) and developed in detail for sudden cracking in Bažant and Cedolin (1979, 1980), and for gradual strain softening in Bažant (1982) and Bažant and Oh (1983).

The basic idea in the crack band model is that the damage propagates as a band whose width has a certain minimum characteristic value  $h_c$ . For a given constitutive law of concrete,  $h_c$  depends on the postpeak strain-softening curve. The element size must be determined accordingly. In most cases, when the damage region (crack band) propagates inside a finite-element mesh, its width will be equal to the size of the elements in the direction perpendicular to the middle surface of the crack band. Therefore, the element size in such a direction must be equal to  $h_c$ .

The crack band approach has been introduced and extensively used for analysis of tensile fracture. As already mentioned, the propagation of a region of compressive strain-softening damage is driven by energy release in the structure, and in this sense it is a phenomenon analogous to the propagation of tensile cracking. Thus, in terms of strain localization, the same arguments as those made when dealing with tensile failure apply also to the case of compressive failure.

Determining the proper band width (and thus the element size) to be adopted in finite-element analysis is not a simple task. Often this must be done empirically. For the present analysis of concrete columns, the element size was empirically determined as the element size that gives accurate results for one of the nine specimens to be analyzed (namely, the small specimen of intermediate slenderness, S2). This size has then been kept constant for the remaining computations. This guarantees consistency throughout the analysis and makes possible a meaningful comparative study of the results obtained for different specimen sizes. The element size in the direction normal to the expected plane of propagation of the damage region (the horizontal plane) is taken to be approximately 1.7 times the maximum aggregate size.

The crack band model involves not only a restriction on the element size but also a prescription for what to do if such a size is inconvenient, e.g., so small as compared with the structure size that the number of elements would be forbiddingly large. This prescription allows changing the element size if the stress-strain relation is adjusted as a function of element size in a manner that ensures that the results to be the same as those with the correct element size and the unadjusted stress-strain relation. In the present computations, however, the number of finite elements was manageable, and so this feature of the crack band model was not invoked.

One last comment needs to be made on the effect that the orientation of the elements in the mesh might have on the results. Whenever a damage region propagates through the elements of a finite-element mesh, there is a tendency for it to

follow the mesh lines. A comparison of results obtained for different meshes, with different orientation of the elements, would be needed, in order to capture accurately the propagation of the damage into the column. However, the main focus of this paper is on the size effect and, thus, during each computation, what is needed is the nominal strength,  $\sigma_N = P/D^2$ , calculated from the peak load. The peak is reached when the embedded reinforcing bars buckle, after softening of the surrounding concrete. Therefore, upon reaching the peak load, the damage region has not yet propagated deep inside the column. For this reason, the mesh adopted for the computation seems to be sufficient to capture the response of the columns up to the peak. An improved prediction of the propagation of the damage would be essential to capture accurately the postpeak behavior of the column, which is beyond the scope of this paper.

## MICROPLANE MODEL

For concrete, the material model is based on the microplane approach, which is proven to yield good results for both small and finite strain conditions.

With the microplane model approach (Bažant 1984b; Bažant and Oh 1985; Bažant and Prat 1987, 1988a,b; Carol and Bažant 1997; Bažant et al. 2000b; Caner and Bažant 2000), the constitutive behavior of materials is characterized by relations between the stress and strain vectors acting on planes of all possible orientations within the material, called the microplanes, and the macroscopic strain and stress tensors are determined from the contributions of the stress and strain components on all the microplanes. The orientation of a microplane is characterized by the unit normal  $\mathbf{n}$  of components  $n_i$  (indices  $i$  and  $j$  refer to the components in Cartesian coordinates  $x_i$ ). In the formulation with kinematic constraint, which makes it possible to describe softening in a stable manner, the strain vector  $\epsilon_N$  on the microplane (Fig. 3) is the projection of the macroscopic strain tensor  $\epsilon_{ij}$ . So the components of this vector are  $\epsilon_{Ni} = \epsilon_{ij}n_j$ . The normal strain on the microplane is  $\epsilon_N = n_i\epsilon_{Ni}$ , that is

$$\epsilon_N = N_{ij}\epsilon_{ij}; \quad N_{ij} = n_in_j \quad (1)$$

where repeated indices imply summation over  $i = 1, 2, 3$ . The mean normal strain, called the volumetric strain  $\epsilon_V$ , and the deviatoric strain  $\epsilon_D$  on the microplane can also be introduced, defined as follows (for small strains):

$$\epsilon_V = \epsilon_{kk}; \quad \epsilon_D = \epsilon_N - \frac{1}{3}\epsilon_V = \frac{2}{3}(\epsilon_N - \epsilon_S) \quad (2)$$

where  $\epsilon_S$  = spreading strain = mean normal strain in microplane.  $\epsilon_S$  characterizes the lateral confinement of the micro-

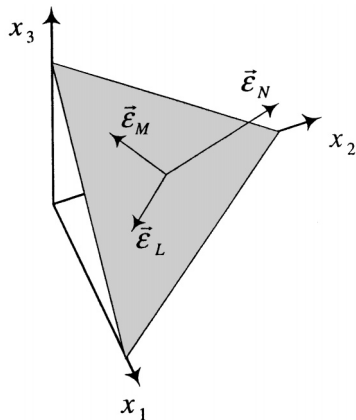


FIG. 3. Strain Components on Microplane

plane and the creation of splitting cracks normal to the microplane. Considering  $\epsilon_V$  and  $\epsilon_D$  (or  $\epsilon_S$ ) is useful when dealing with the effect of lateral confinement on compression failure and when the volumetric-deviatoric interaction observed for a number of cohesive frictional materials, such as concrete, needs to be captured.

To characterize the shear strains on the microplane (Fig. 3), we need to define two coordinate directions  $M$  and  $L$ , given by two orthogonal unit coordinate vectors  $\mathbf{m}$  and  $\mathbf{l}$  of components  $m_i$  and  $l_i$  lying on the microplane. To minimize directional bias of  $\mathbf{m}$  and  $\mathbf{l}$  among microplanes, we alternate among choosing vectors  $\mathbf{m}$  to be normal to axis  $x_1$ ,  $x_2$ , or  $x_3$ .

The magnitudes of the shear strain components on the microplane in the directions of  $\mathbf{m}$  and  $\mathbf{l}$  are  $\epsilon_M = m_i(\epsilon_{ij}n_j)$  and  $\epsilon_L = l_i(\epsilon_{ij}n_j)$ . Because of the symmetry of tensor  $\epsilon_{ij}$ , the shear strain components may be written as follows (Bažant et al. 1996, 2000b):

$$\epsilon_M = M_{ij}\epsilon_{ij}; \quad \epsilon_L = L_{ij}\epsilon_{ij} \quad (3)$$

in which the following symmetric tensors are introduced:

$$M_{ij} = (m_in_j + m_jn_i)/2; \quad L_{ij} = (l_in_j + l_jn_i)/2 \quad (4)$$

Once the strain components on each microplane are obtained, the stress components are updated through microplane constitutive laws, which can be expressed in algebraic or differential form.

If the kinematic constraint is imposed, the stress components on the microplanes are equal to the projections of the macroscopic stress tensor  $\sigma_{ij}$  only in some particular cases, when the microplane constitutive laws are specifically prescribed so that this condition be satisfied. This happens, for example, in the case of elastic laws at the microplane level, defined with elastic constants chosen so that the overall macroscopic behavior is the usual elastic behavior (Carol and Bažant 1997). In general, the stress components determined independently on the various planes will not be related to one another in such a manner that they can be considered as projections of a macroscopic stress tensor. Thus, the static equivalence or equilibrium between the microlevel stress components and macrolevel stress tensor must be enforced by other means. This can be accomplished by application of the principle of virtual work, yielding

$$\sigma_{ij} = \frac{3}{2\pi} \int_{\Omega} \sigma_N n_i n_j d\Omega + \frac{3}{2\pi} \int_{\Omega} \frac{\sigma_{Tt}}{2} (n_i \delta_{rj} + n_j \delta_{ri}) d\Omega \quad (5)$$

where  $\Omega$  = surface of a unit hemisphere. Eq. (5) follows from the equality of the virtual work inside a unit sphere and on its surface, rigorously justified by Bažant et al. (1996). The integration in (5) is performed numerically by an optimal Gaussian integration formula for spherical surface using a finite number of integration points on the surface of the hemisphere. Such an integration technique corresponds to considering a finite number of microplanes, one for each integration point. A formula consisting of 28 integration points is given by Stroud (1971). Bažant and Oh (1986) developed a more efficient and about equally accurate formula with 21 integration points and studied the accuracy of various formulas in different situations.

The microplane model for concrete is the result of almost two decades of studies by Bažant and coworkers. The version adopted for the analysis presented in this paper is referred to as M4, and a complete description of it can be found in Bažant et al. (1999). Model M4 is formulated by use of simple one-to-one relations between one stress component and the associated strain component. Except for a frictional yield surface, cross dependencies are not accounted for explicitly, but appear in the model as result of the interaction among planes.

Each constitutive relationship at the microplane level is expressed by introducing stress-strain boundaries (strain-dependent yield limits): the response is elastic until any of the boundaries is reached; after that, the stress drops at constant strain to the boundary.

The model parameters are divided into a few adjustable ones (only four are needed) and many nonadjustable ones (of which twenty are used), common to all concretes. Bažant et al. (1999) provide an efficient procedure to identify the model parameters in a systematic way from test data. Creep and rate-effect have also been introduced in M4, but are neglected in this study. A finite strain analysis is necessary in order to capture buckling, particularly the so-called  $P-\delta$  effect. The basic formulation of the microplane model presented here (valid for the small strains range) is therefore extended to the finite strain range, following Bažant et al. (2000a). Considering finite strains automatically takes into account not only the overall buckling of the column but also the local buckling of steel bars embedded in concrete, if it is assumed that the resistance to the buckling of bars is provided mainly by the stiffness of the embedment and not by the bending stiffness of the bars themselves, which is neglected.

## RESULTS OF ANALYSIS AND COMPARISONS WITH TESTS

Figs. 4–6 show the meshes used for specimens of three different slendernesses. Each figure exhibits three specimens with the same cross section and three different slendernesses. For each specimen type, the figure shows separately the finite elements used to model the reinforcement (including top and bottom steel plates), the undeformed mesh of the whole specimen and the deformed mesh at the end of the loading process. The specimen sizes (cross-section sides) are  $D = 12.7$ , 25.4, and 50.8 mm (0.5, 1, and 2 in.) for Figs. 4–6, respectively.

The size effect is determined by comparing the results ob-

tained for geometrically similar specimens with constant slenderness  $\lambda$  and varying size  $D$ . Fig. 7(a) shows the computed load-displacement diagrams for the three specimens characterized by slenderness  $\lambda = 19.2$ . The same figure also indicates the peak loads obtained experimentally, and also what the peak loads would be, for the middle and large specimens, if they were simply scaled with size from the computed peak load of the small specimen, ignoring the size effect (which corresponds to plastic limit analysis underlying the current codes). It can be clearly seen that the actual and computed values of the peak loads for the larger specimens are significantly less than the values that would be expected without the size effect. Similar plots for the cases for  $\lambda = 35.8$  and  $\lambda = 52.5$  are given in Figs. 7(b and c). In these figures, the specimen labels, S, M, and L mean the small, middle, and large cross section, and the subsequent numbers, 1, 2, and 3 mean the low, middle, and high slenderness, respectively.

The best way to discuss systematically the results of finite-element analysis is, however, by plotting them on standard size effect plots of  $\log \sigma_N$  versus  $\log D$ . Such plots are shown in Fig. 2, for the three groups of specimens, again grouped by slenderness.

Based on previous theoretical arguments of general validity (Bažant and Cedolin 1991; Bažant and Chen 1997; Bažant 1997), the size effect should be described by the following approximate size-effect law proposed by Bažant (1984a):

$$\sigma_N = Bf'_t(1 + \beta)^{-1/2}, \quad \beta = D/D_0 \quad (6)$$

in which  $Bf'_t$  and  $\beta$  are two empirical constants (the tensile strength  $f'_t$ , is introduced merely for convenience, to make  $B$  nondimensional). For comparison, Fig. 2 shows also the experimental results and their optimal fits by this size effect law.

The experimental evidence and theoretical arguments (Bažant and Planas 1999) show that the dependence of  $\log \sigma_N$  on  $\log D$  for geometrically similar structures is such that it approaches a horizontal asymptote for small sizes and a straight

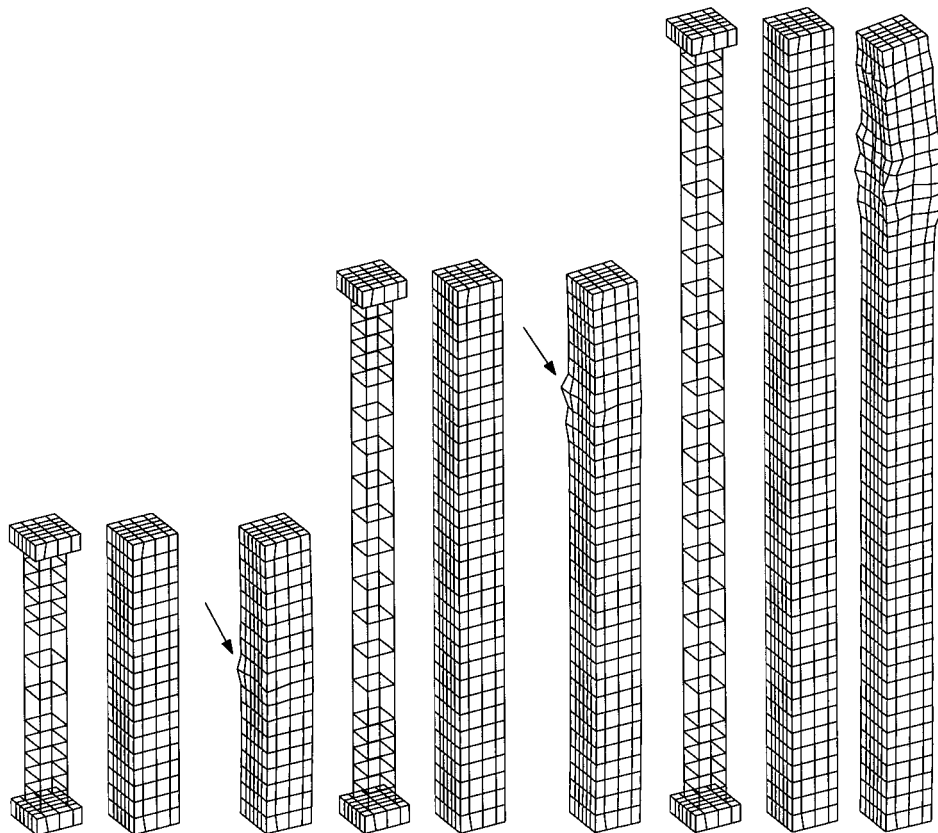
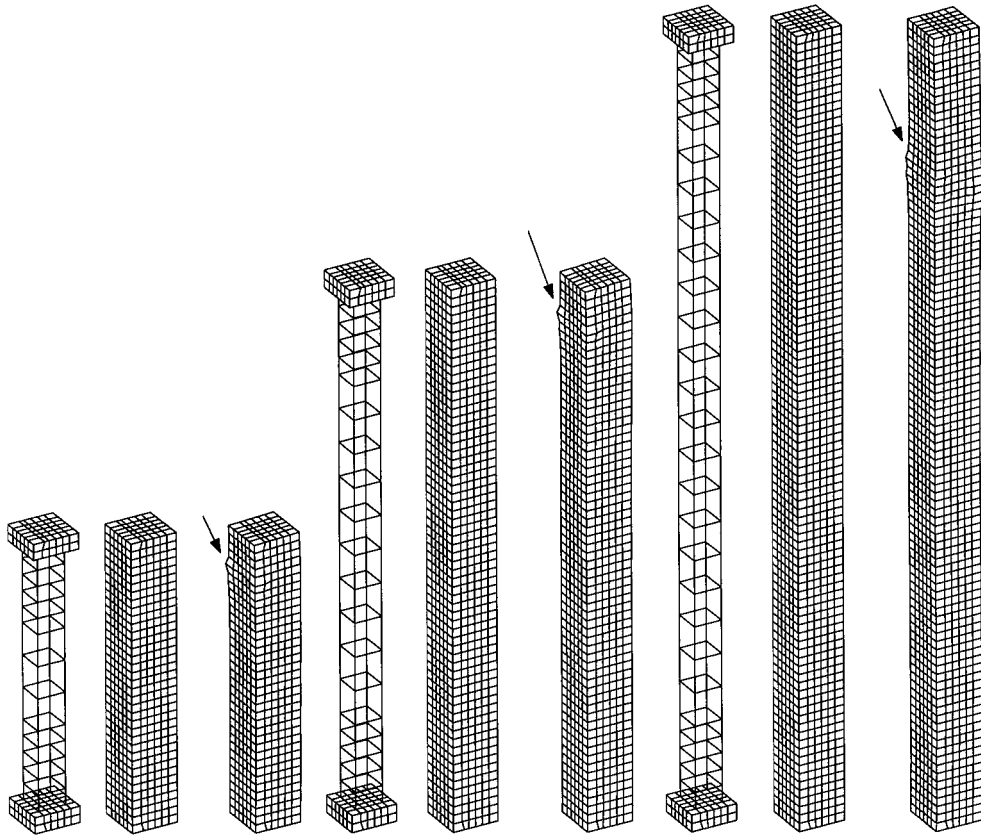
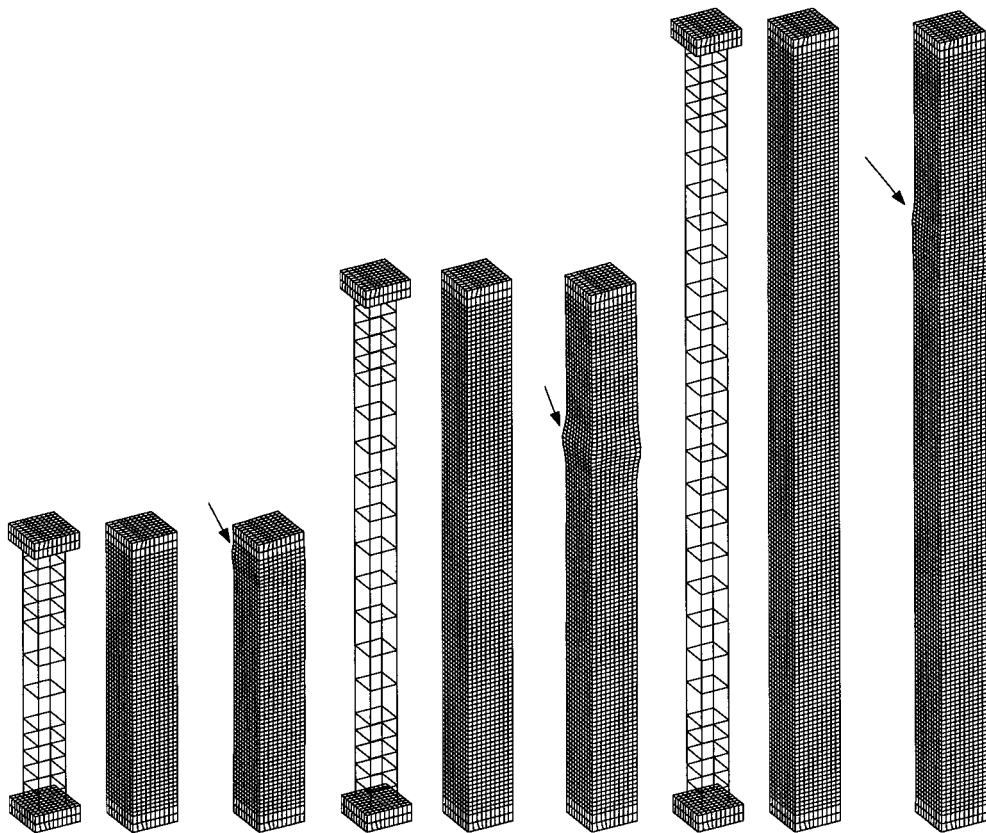


FIG. 4. Undeformed and Deformed Meshes Used for Computations of Specimens of Size  $D = 12.7$  mm (0.5 in.)



**FIG. 5.** Undeformed and Deformed Meshes Used for Computations of Specimens of Size  $D = 25.4$  mm (1 in.)



**FIG. 6.** Undeformed and Deformed Meshes Used for Computations of Specimens of Size  $D = 50.8$  mm (2 in.)

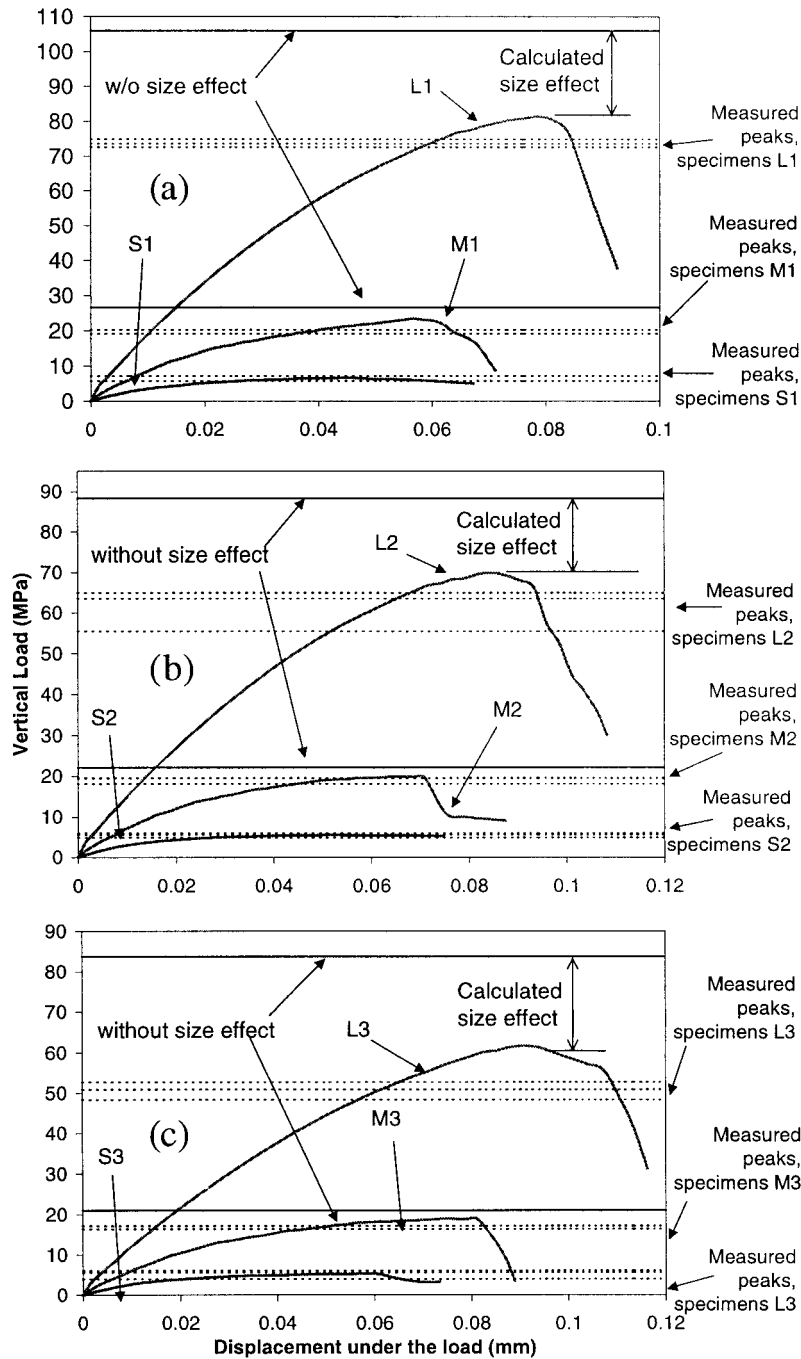


FIG. 7. Computed Load-Displacement Curves for Specimens with Slendernesses  $\lambda = 19.2, 35.8, \text{ and } 52.5$

line asymptote of slope  $-1/2$  for  $D \rightarrow \infty$ . For  $D \rightarrow \infty$ , the size of the fracture process zone, as compared with the size of the structure, is so small that the behavior of the structure approaches that predicted by linear elastic fracture mechanics. When the results of finite-element analysis are shown in the bilogarithmic plot, it can be seen that a smooth curve interpolating the three points for the three specimen sizes has negative curvature, in general agreement with the theory. This shows that the mean trend of the size effect is captured in a realistic way.

Quantitatively, the results are satisfactory too, although the predicted size effect is slightly less strong than that observed experimentally. In particular, observe that the approximation seems to worsen slightly with an increasing slenderness. There are two reasons to which this discrepancy can be attributed. First, the present analysis assumes a perfect bond between the steel bars and concrete. Since smooth steel bars had to be used

in the tests, debonding and pull-out might have played some role in reducing the nominal strength with increasing size. Obviously, debonding cannot be captured under the assumptions made for the present analysis. Second, the crack band model must be expected to give results too stiff, because the mesh could not be conveniently laid out so that the mesh lines would follow the boundary of the softening damage zone (this is known as "stress locking"). Also, the crack band model cannot distinguish the mutual amplification and shielding of interacting microcracks of different orientations (Bažant 1994). Doubtless, a nonlocal formulation, using finite elements at least three times smaller, would yield more accurate results. However, the number of finite elements required would increase 27 times, which would call for a more powerful computer than that affordable with the available funding.

Size effect testing of real size columns with real size aggregates had also begun (Abusiaf et al. 1996). The results so

far agree with Bažant and Xiang's (1997) analysis. However, they are limited in the range and scope to serve as a check on the present model.

## COMPARISON WITH SIMPLIFIED METHOD OF ANALYSIS

Bažant and Xiang (1997) proposed a method of analysis of the size effect in compression failure based on the calculation of the change in the strain energy stored in the columns corresponding to an assumed mechanism of failure. Recognizing that the compression failure is triggered by the formation of axial splitting cracks, they assumed that the principal mechanism of compression failure is sideways propagation of a band of parallel axial splitting cracks in a direction either inclined or orthogonal with respect to the direction of compression. Failure occurs when the microslabs of material between the axial cracks buckle. Bažant and Xiang assumed that the length of the axial cracks is a material property to be determined empirically, while their spacing is unknown. They proposed two ways by which the effect of column slenderness can be taken into account: (1) by introducing a magnification factor for the lateral deflection at midheight based on the theory of stability; and (2) by calculating the additional energy release engendered by slenderness. The two methods yield similar results.

The size effect predicted by Bažant and Xiang's (1997) method is slightly more pronounced than that obtained with the present finite-element analysis and captures slightly more accurately the behavior observed in Bažant and Kwon's (1994) tests.

An interesting result of Bažant and Xiang's (1997) analysis is that the asymptotic size effect in compression failure for large sizes is predicted to give  $\sigma_N \propto D^{-2/5}$ , and thus to be weaker than in LEFM (for which  $\sigma_N \propto D^{-1/2}$ ). Exponent  $-2/5$  was also obtained for the breakout of boreholes in rock (Bažant et al. 1993). The difference in exponents is caused by the fact that the energy release that causes size effect is assumed to be maximized with respect to the spacing of the axial splitting cracks, which leads to the conclusion that the spacing is not constant, but increases as  $D^{0.1}$  [Bažant and Xiang (1996), where equation (17) has a misprint]. It is not clear whether this maximization should be used because the minimum spacing of main cracks is limited by the maximum aggregate size. Therefore, a constant spacing is assumed here. The size range of test data is not sufficient to ascertain the asymptotic slope of the size effect curve. Microstructure simulation with some realistic particle model could provide a clue.

## CONCLUSIONS

1. When geometrically similar columns of different sizes, made of the same concrete, are considered, all the current design codes predict the same nominal strength  $P/D^2$ , while in reality, tied reinforced concrete columns exhibit a strong size effect of fracture mechanics type. The experimental results and the present numerical analysis based on the crack band concept confirm that compressive failure of concrete cannot be described by strength criteria, but is caused by the release of strain energy stored in the structure, in a similar way as in tensile failure.
2. As shown by the present results, a finite-element analysis carried out with the microplane model and based on the crack-band concept can capture the size effect in failure of reinforced concrete columns under eccentric load.
3. The predicted reduction in nominal strength with increasing size is, however, slightly less than that observed experimentally. This may probably be attributed to the as-

sumption of perfect bond between concrete and steel. Debonding presumably plays a role contributing to a faster reduction of nominal stress with increasing size. Such an aspect of the overall phenomenon cannot be captured under the assumptions made for the present analysis. A second reason for the discrepancy between experimental and computational results is probably the fact that the crack band model is too stiff when the damage band does not propagate along the mesh lines. The nonlocal approach would avoid that, but a far larger number of finite elements would be required.

## REFERENCES

- Abusiaf, H. F., Sener, S., and Barr, B. I. G. (1996). "Size effects in plain and reinforced concrete columns." *Rep.*, Div. of Civil Engrg., University of Wales, Cardiff, U.K.
- Batdorf, S. B., and Budiansky, B. (1949). "A mathematical theory of slip based on the concept of slip." *NACA TN1871*, April.
- Bažant, Z. P. (1976). "Instability, ductility, and size effect in strain softening concrete." *J. Engrg. Mech. Div.*, ASCE, 102(2), 331–344.
- Bažant, Z. P. (1982). "Crack band model for fracture of geomaterials." *Proc., 4th Int. Conf. on Numer. Methods in Geomech.*, Z. Eisenstein, ed., University of Alberta, Edmonton, 3, 1137–1152.
- Bažant, Z. P. (1984a). "Size effect in blunt fracture: concrete, rock, metal." *J. Engrg. Mech.*, ASCE, 110(4), 518–535.
- Bažant, Z. P. (1984b). "Chapter 3: Microplane model for strain controlled inelastic behavior." *Mechanics of engineering materials*, C. S. Desai and R. H. Gallagher, eds., Wiley, London, 45–59.
- Bažant, Z. P. (1991). "Why continuum damage is nonlocal: micromechanics arguments." *J. Engrg. Mech.*, ASCE, 117(5), 1070–1087.
- Bažant, Z. P. (1994). "Nonlocal damage theory based on micromechanics of crack interactions." *J. Engrg. Mech.*, ASCE, 120(3), 593–617.
- Bažant, Z. P., et al. (2000a). "Large-strain generalization of microplane model for concrete and application." *J. Engrg. Mech.*, ASCE, 126(9), 971–980.
- Bažant, Z. P., Belytschko, T. B., and Chang, T.-P. (1984). "Continuum theory for strain-softening." *J. Engrg. Mech.*, ASCE, 110(12), 1666–1692.
- Bažant, Z. P., Caner, F. C., Carol, I., Adley, M. D., and Akers, S. A. (2000b). "Microplane model M4 for concrete. I: Formulation with work-conjugate deviatoric stress." *J. Engrg. Mech.*, ASCE, 126(9), 944–953.
- Bažant, Z. P., and Cedolin, L. (1980). "Fracture mechanics of reinforced concrete." *J. Engrg. Mech. Div.*, ASCE, 106(6), 1287–1306.
- Bažant, Z. P., and Cedolin, L. (1979). "Blunt crack band propagation in finite element analysis." *J. Engrg. Mech. Div.*, ASCE, 105(2), 297–315.
- Bažant, Z. P., and Cedolin, L. (1991). *Stability of structures: elastic, inelastic, fracture and damage theories*, Oxford University Press, New York.
- Bažant, Z. P., Cedolin, L., and Tabbara, M. R. (1991). "New method of analysis for slender columns." *ACI Struct. J.*, 88(4), 391–401.
- Bažant, Z. P., and Chen, E.-P. (1997). "Scaling of structural failure." *Appl. Mech. Reviews*, 50(10), 593–627.
- Bažant, Z. P., Kim, J.-J. H., and Brocca, M. (1999). "Finite strain tube-squash test of concrete at high pressures and shear angles up to 70 degrees." *ACI Mat. J.*, 96(5), 580–592.
- Bažant, Z. P., and Kwon, Y. K. (1994). "Failure of slender and stocky reinforced concrete columns: tests of size effect." *Mat. and Struct.*, 27, 79–90.
- Bažant, Z. P., and Lin, F.-B. (1988a). "Nonlocal smeared cracking model for concrete fracture." *J. Struct. Engrg.*, ASCE, 114(11), 2493–2510.
- Bažant, Z. P., and Lin, F.-B. (1988b). "Non-local yield limit degradation." *Int. J. for Numer. Methods in Engrg.*, 26, 1805–1823.
- Bažant, Z. P., Lin, F.-B., and Lippmann, H. (1993). "Fracture energy release and size effect in borehole breakout." *Int. J. Numer. Analytical Methods in Geomech.*, 17, 1–14.
- Bažant, Z. P., and Oh, B. H. (1983). "Crack band theory for fracture of concrete." *Mat. and Struct.*, 16, 155–177.
- Bažant, Z. P., and Oh, B.-H. (1986). "Efficient numerical integration on the surface of a sphere." *Zeitschrift für angewandte Mathematik und Mechanik (ZAMM)*, Berlin, 66(1), 37–49.
- Bažant, Z. P., and Ožbolt, J. (1990). "Nonlocal microplane model for fracture, damage and size effect in structures." *J. Engrg. Mech.*, ASCE, 116(11), 2485–2505.
- Bažant, Z. P., and Ožbolt, J. (1992). "Compression failure of quasibrittle

- material: nonlocal microplane model." *J. Engrg. Mech.*, ASCE, 118(3), 540–556.
- Bažant, Z. P., and Pijaudier-Cabot, G. (1988). "Nonlocal continuum damage, localization instability and convergence." *J. Appl. Mech.*, 55, 287–290.
- Bažant, Z. P., and Pijaudier-Cabot, G. (1989). "Measurement of characteristic length of nonlocal continuum." *J. Engrg. Mech.*, ASCE, 115(4), 755–767.
- Bažant, Z. P., and Planas, J. (1998). *Fracture and size effect in concrete and other quasibrittle materials*, CRC Press, Boca Raton, Fla.
- Bažant, Z. P., and Prat, P. C. (1988). "Microplane model for brittle plastic materials. II: Verification." *J. Engrg. Mech.*, ASCE, 114(10), 1689–1699.
- Bažant, Z. P., and Xi, Y. (1991). "Statistical size effect in quasi brittle structures. II: Nonlocal theory." *J. Engrg. Mech.*, ASCE, 117(11), 2623–2640.
- Bažant, Z. P., Xi, Y., and Reid, S. G. (1991). "Statistical size effect in quasi brittle structures. I: Is Weibull theory applicable?" *J. Engrg. Mech.*, ASCE, 117(11), 2609–2622.
- Bažant, Z. P., and Xiang, Y. (1997). "Size effect in compression fracture: splitting crack band propagation." *J. Engrg. Mech.*, ASCE, 123(2), 162–172.
- Bieniawski, Z. T. (1974). "Estimating the strength of rock materials." *J. South African Inst. of Min. Metal.*, 74, 312–320.
- Blanks, R. F., and McNamara, C. C. (1935). "Mass concrete tests in large cylinders." *J. Am. Concrete Inst.*, 31, 280–303, 1935.
- Brocca, M., and Bažant, Z. P. (2001). "Microplane finite element analysis of tube-squash test of concrete with shear angles up to 70 degrees." *Int. J. for Numer. Methods in Engrg.*, in press.
- Caner, F. C., and Bažant, Z. P. (2000). "Microplane model M4 for concrete. II: Algorithm and calibration." *J. Engrg. Mech.*, ASCE, 126(9), 954–961.
- Carol, I., and Bažant, Z. P. (1997). "Damage and plasticity in microplane theory." *Int. J. Solids and Struct.*, 34(29), 3807–3835.
- Cotterell, B. (1972). "Brittle fracture in compression." *Int. J. Fract. Mech.*, 8(2), 195–208.
- Eringen, A. C. (1965). "Theory of micropolar continuum." *Proc., 9th Midwestern Mech. Conf.*, 23–40.
- Gonnermann, H. F. (1925). "Effect of size and shape of test specimen on compressive strength of concrete." *Proc., ASTM*, ASTM, West Conshohocken, Pa., 25, 237–250.
- Hoek, E., and Bieniawski, Z. J. (1965). "Brittle fracture propagation in rock under compression." *Int. J. Fracture Mech.*, 1, 137–155.
- Ingraffea, A. R. (1997). "Discrete fracture propagation in rock: laboratory tests and finite element analysis." PhD thesis, University of Colorado, Boulder, Colo.
- Jirásek, M., and Bažant, Z. P. (1994). "Localization analysis of nonlocal model based on crack interactions." *J. Engrg. Mech.*, ASCE, 120(7), 1521–1542.
- Jishan, X., and Xixi, H. (1990). "Size effect on the strength of a concrete member." *Engrg. Fracture Mech.*, 35, 687–696.
- Kröner, E. (1967). "Elasticity theory of materials with long-range cohesive forces." *Int. J. Solids and Struct.*, 3, 731–742.
- Kunin, I. A. (1968). "The theory of elastic media with microstructure and the theory of dislocations." *Mechanics of generalized continua*, E. Kröner, ed., Springer Verlag, Berlin, 321–328.
- Marti, P. (1989). "Size effect on double punch tests on concrete cylinders." *ACI Mat. J.*, 86(6), 597–601.
- McGregor, J. G. (1988). *Reinforced concrete: mechanics and design*, Prentice-Hall, Englewood Cliffs, N.J.
- Nilson, A. H., and Winter, G. (1986). *Design of concrete structures*, 10th Ed., McGraw-Hill, New York.
- Ožbolt, J., and Bažant, Z. P. (1996). "Numerical smeared fracture analysis: nonlocal microcrack interaction approach." *Int. J. for Numer. Methods in Engrg.*, 39, 635–661.
- Pijaudier-Cabot, G., and Bažant, Z. P. (1987). "Nonlocal damage theory." *J. Engrg. Mech.*, ASCE, 113(10), 1512–1533.
- Planas, J., and Elices, M. (1993). "Asymptotic analysis of cohesive crack. I: Theoretical background." *Int. J. Fracture*, 55, 153–177.
- Planas, J., Elices, M., and Guinea, G. V. (1994). "Cohesive cracks as a solution of a class of nonlocal models." *Fracture and damage of quasi-brittle structures*, Z. P. Bažant, Z. Bittnar, M. Jirásek, and J. Mazars, eds., E & FN Spon, London, 131–144.
- Paul, B. (1968). "Macroscopic criteria for plastic flow and brittle fracture." *Fracture, an advanced treatise*, Vol. 2, H. Liebowitz, ed.,
- Stroud, A. H. (1971). *Approximate calculation of multiple integrals*, Prentice-Hall, Englewood Cliffs, N.J.
- Taylor, G. I. (1938). "Plastic strain in metals." *J. Inst. of Metals*, 63, 307–324.
- van Mier, J. G. M. (1986). "Multiaxial strain softening in concrete." *Mat. and Struct.*, Paris, 19, 179–200.